




Curvature-dependent adhesion of vesicles

Kun Li ¹, Cunjing Lv ^{1,2,3,*} and Xi-Qiao Feng ^{1,2,4}

¹*Institute of Biomechanics and Medical Engineering, Applied Mechanics Laboratory, Department of Engineering Mechanics, Tsinghua University, Beijing 100084, China*

²*Center for Nano and Micro Mechanics, Tsinghua University, Beijing 100084, China*

³*State Key Laboratory of Tribology in Advanced Equipment (SKLT), Tsinghua University, Beijing 100084, China*

⁴*Laboratory of Flexible Electronics Technology, Tsinghua University, Beijing 100084, China*



(Received 14 April 2022; accepted 9 January 2023; published 7 February 2023)

The morphology and motion behavior of a cell are highly influenced by its external biological, chemical, and physical stimuli, and geometric confinement. In this paper, it is revealed that the mean curvature of the substrate significantly influences the adhesion of vesicles. By employing the variational method and investigating the Helfrich free energy, the configuration of axisymmetric vesicles adhered to curved spherical substrates is obtained theoretically. Moreover, numerical simulations based on the finite element method are also carried out to investigate the adhesion of vesicles on curved substrates with complex shapes. It is found that for a fixed area of a vesicle, its total free energy depends mainly on the mean curvature of the adhesion region but is insensitive to the specific shape of the substrate, and the total free energy monotonically decreases with the increase in the mean curvature. In addition, possible biological significances of the curvature-dependent adhesion, such as the shape of the cell and antibiofouling, are discussed. This study may deepen our understanding of the underlying mechanisms of adhesion in cellular activities.

DOI: [10.1103/PhysRevE.107.024405](https://doi.org/10.1103/PhysRevE.107.024405)

I. INTRODUCTION

Adhesion plays an extremely important role in physiological and pathological activities of cells [1–5]. For example, adhesion greatly contributes to the organization, proliferation, survival, phagocytosis, exocytosis, metabolism, and gene expression of cells [1,6–8]. Moreover, adhesion is crucial in the biomedical and biotechnology fields [9,10]. For example, cells are fixed on a substrate or extracellular matrix for highly efficient medicine transport [11], and biotechnical applications also require the adhesion of membranes to a substrate [11,12]. Recent studies suggest that the geometry of the substrate affects the adhesion and the realization of the functionality of cells. In addition, cells take different morphologies when adhering to concave and convex substrates [3], and most cells tend to migrate from convex regions to concave valleys for stronger adhesion [2]. Therefore, a rational morphological design of substrates may suppress the adhesion of cells and retard biofouling [13].

In recent years, the adhesion of cells on curved substrates has attracted much attention due to its scientific significance and potential applications. Seifert and Lipowsky introduced the contact potential to describe the intensity of the adhesion energy between a vesicle and a flat substrate [14–16]. From the geometrical point of view, differential operators and integral theorems were applied to predict the equilibrium configurations of vesicles adhered to flat and curved substrates [17–21]. Das and Du investigated the adhesion of vesicles on

curved substrates. They found that concave substrates favor vesicle adhesion in comparison with convex substrates, and found that the transition from a free vesicle to a bound state depends significantly on the substrate shape [17]. To investigate the situation with a nonaxisymmetric shape, Zhang *et al.* developed an adaptive finite element method (FEM) that can characterize the adhesion of vesicles on substrates with complex shapes, and they also found that concave substrates favor adhesion [22]. Moreover, Shi *et al.* investigated the pulling of a vesicle adhered to curved substrates, and correlated the external force and the displacement of the vesicle to the substrate shape and interaction potential [23]. The adhesion behavior of a vesicle on a curved soft substrate was also theoretically studied, and different equilibrium states of wrapping of the vesicle depending on the work of adhesion and bending stiffness were reported [6,24]. Besides the study of individual vesicles, it was recently found that the substrate curvature can regulate both the migration mode and density fluctuation of the collective cell population [25–27]. Besides the substrate curvature, the role of the spontaneous curvature and local curvature of free vesicles in the engulfment of nanoparticles was investigated by Agudo-Canalejo and Lipowsky [28,29]. They discovered that partially engulfed nanoparticles can be pulled towards the membrane segments with lower and higher mean curvatures if the particles originate from the exterior and interior solutions, corresponding to endo- and exocytosis, respectively.

Despite these previous efforts, there is still a lack of comprehensive understanding of the influence of substrate curvature on the adhesion of vesicles. Recent *in vitro* experiments showed that the adhesion, migration, and differentiation behaviors of cells are closely related to the substrate curvature

*cunjinglv@tsinghua.edu.cn

[2,3,27]. Recently, Pieuchot *et al.* reported a cellular ability and termed it as “curvotaxis” [2], suggesting that cells are able to respond to cell-scale curvature variations, and the adherent cells avoid convex regions during their migration and position themselves in concave valleys. However, the underlying physics remains obscure. The above interesting results motivate us to perform the current study from a theoretical point of view. We devote this work to clarifying how curved substrates affect the adhesion behavior of the vesicle. Specifically, we will show that the mean curvature of the adhesion region plays a significant role. For curved substrates with different shapes (such as spherical, cylindrical, conical, saddle-shaped, and many other complex shapes), the vesicle may exhibit similar adhesion behaviors when the local adhesion regions between the vesicle and the substrate have the same mean curvature.

These questions are reminiscent of the wetting of droplets and particles on curved solid substrates and fluid interfaces, where the curvature-driven mechanism has been well quantified in a broad range of interfacial systems, such as spontaneous transport of droplets on curved solid substrates [30–33] and liquid-vapor interfaces [34], particles at liquid-vapor [35] and solid-vapor interfaces [36], and bubbles at the liquid-vapor interfaces [34]. Despite these systematic investigations, the droplets, bubbles and liquid-vapor interfaces have negligible stiffness [37], meaning that the adhesion systems were much simpler than the adhesion of vesicles. For a vesicle, besides surface tension, stiffness may have an important influence on adhesion, which makes the analysis intractable. Moreover, the manner to handle the question of an adhering vesicle is remarkably different from that of a wetting drop. For a drop, surface tension σ is usually constant, for given parameters such as the droplet volume V , the strength of adhesion (which could be characterized by employing the contact angle θ), and the specific shape of the substrate, other quantities of interest can be simply solved, such as the total energy of the drop E_{tot} (and its components), the contact area A_c , and the free area (liquid-vapor area) A_f , as well as the drop shape. However, this is not the case for a vesicle. To theoretically solve the profile of an adhering vesicle, we usually employ the variational method [38] and Helfrich free energy [39], in which some conservation relationships must be given in advance. Usually, we assume that the vesicle either has a constant area or a constant volume [6,18,24]. Considering that the vesicle consists of a certain amount of lipid molecules, we assume that its total area A stays constant. In this case, the vesicle volume V will be adjusted through the osmotic pressure when adhering to different substrates. Detailed discussions will be given in the following sections, from which we will see the surface tension σ and volume V of the vesicle are determined by given physical parameters (such as spontaneous curvature c_0 , stiffness k_c , contact potential w , and pressure difference ΔP), as well as the mean curvature κ of the adhesion region. Therefore, clarification of the unknown influences of the substrate mean curvature on the adhesion of a vesicle might shed light on fundamental understandings of the adhesion and bring great prospects for biotechnology applications.

In this paper, the influence of the substrate mean curvature on the adhesion behavior of a vesicle is investigated. Based on the variational method [38] and Helfrich free

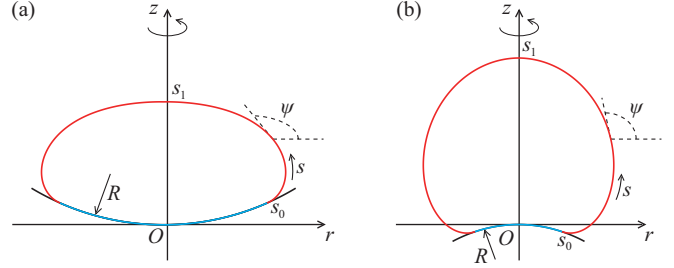


FIG. 1. Configuration of an axisymmetric vesicle adhered to spherical convex (a) and concave (b) substrates in the cylindrical coordinate system, where r and z are the radial and axial coordinates, respectively. s represents the arc length parameter of the vesicle, and the positive direction is denoted by the associated arrows. ψ represents the angle between the tangent line at an arbitrary point (r, z) and the horizontal line (i.e., the direction along the r axis). R and $\kappa = \pm 1/R$ are defined as the curvature radius and the curvature of the spherical substrate, respectively. Here, R has a positive value, and the plus and minus signs in κ are defined for the cases of [(a),(b)], respectively.

energy [39], we theoretically derive the governing equations and boundary conditions of axisymmetric adhering vesicles on curved substrates, and the configurations are numerically solved by employing a shooting method. Under given values of the physical parameters such as the stiffness, spontaneous curvature, contact potential, and osmotic pressure difference (between the inside and outside) of the vesicle, the surface tension and the volume are determined by these physical parameters and will change with the mean curvature of the adhesion region. An important finding is that the free energy of an adhering vesicle depends mainly on the mean curvature of the adhesion region but is insensitive to the specific shape of the substrate. By employing the FEM to study the nonaxisymmetric shape of vesicles adhered to cylindrical, conical, and saddle-shaped substrates, the generality of our findings is verified. Moreover, we find there is a mean curvature-dependent threshold for the detachment of the vesicle from the substrate. We expect this work will deepen our understanding of the cellular adhesion behaviors and find applications to regulate many functions such as motion, morphology, and evolution of the cells.

II. THEORY

A. Model of an adhered vesicle

As shown in Fig. 1, we consider a vesicle adhered to a curved substrate. In the theoretical part, for simplicity, we will focus on an axisymmetric vesicle which is in contact with a spherical rigid substrate surface. Let the positive parameter R denote the curvature radius of the spherical surface and $\kappa = \pm 1/R$ denote its mean curvature, where the plus and minus signs are defined for a spherical concave [Fig. 1(a)] and a spherical convex [Fig. 1(b)] substrate, respectively. In this regard, the vesicle consists of two regimes: the area adhered to the substrate and the free area. In addition, we assume that the vesicle is homogeneous and has uniform physical parameters such as spontaneous curvature, bending stiffness, osmotic pressure, and contact potential. In the adhesion area,

the interaction between the fluid membrane and the substrate is modeled by an effective contact potential w [16,17]. Following the pioneering work of Helfrich [39] and referring to the cylindrical coordinate system shown in Fig. 1, we use s to denote the arc length parameter of the surface profile, and ψ denotes the angle between the tangent line at an arbitrary point (r, z) and the horizontal line, with r and z being the radial and axial coordinates, respectively. In the adhesion region (blue) and the free surface (red), one has $s \in [0, s_0]$ and $s \in [s_0, s_1]$, respectively.

According to the Helfrich free energy theory [39,40], the bending energy density per unit area ϕ of a bilayer vesicle is expressed as

$$\phi = \frac{k_c}{2}(2H - c_0)^2 + k_G K, \quad (1)$$

where k_c and k_G are the bending stiffnesses corresponding to the mean curvature H and the Gaussian curvature K , respectively, and c_0 is the spontaneous curvature [39–41]. The total bending energy of the vesicle is obtained by integrating ϕ over the entire vesicle profile. As shown in Fig. 1, even though the adhesion region and the free surface are two separate parts, they are continuous and smooth at s_0 . In other words, $\psi|_{s_{0-}} = \psi|_{s_{0+}}$, denoting s_{0-} and s_{0+} as the points of s_0 at the adhesion area and the free surface, respectively. However, based on the Gauss-Bonnet theorem [41], the contribution of the Gaussian curvature to the total energy is constant for a closed adhering vesicle. Therefore, the variation of the energy resulting from the Gaussian curvature will be zero and k_G will not be considered in the following analysis.

For axisymmetric vesicles, the cylindrical coordinate system is employed, as shown in Fig. 1. In the following, we consider a vesicle that has a target value A_0 of the total area. Then, the free energy E_{tot} of the vesicle can be written as

$$\begin{aligned} E_{\text{tot}} &= \int_A \phi dA - wA_c + \sigma(A - A_0) + \Delta PV \\ &+ \int_{s_0}^{s_1} [\bar{\mu}(s)(\dot{r} - \cos \psi) + \bar{\eta}(s)(\dot{z} - \sin \psi)] dA \\ &= 2\pi k_c \left[\int_0^{s_0} L_1(\psi) ds + \int_{s_0}^{s_1} L(\psi, \dot{\psi}, r, \dot{r}, z, \dot{z}) ds \right] \\ &- \sigma A_0. \end{aligned} \quad (2)$$

It shows that the free energy consists of several parts: the bending energy $\int_{A_c} \phi dA$ and $\int_{A_f} \phi dA$ in the adhesion area A_c and the free surface A_f , respectively; the surface energy σA_c and σA_f in the two regions, with σ being the surface tension of the vesicle; the adhesion energy $-wA_c$ in the adhesion region,

with w being the contact potential [16,17]; and the volume potential ΔPV , with ΔP being the osmotic pressure difference between the inside and outside of the vesicle [16,17]. Here, $A = A_f + A_c$ is the actual total area of the vesicle during the calculation, and V is the volume of the vesicle. In this work, we will not consider the influence of line tension on the morphology of the vesicle [18,22]. Moreover, $\bar{\mu}(s)$ and $\bar{\eta}(s)$ serve as the Lagrange multipliers to impose the geometric relations $\dot{r} = \cos \psi$ and $\dot{z} = \sin \psi$, where the dot is defined as the derivative to s , i.e., $(\dots)' = d(\dots)/ds$.

In the present work, we assume that the vesicle with a certain number of lipid molecules has a fixed area A_0 . In this regard, we will see that the surface tension σ will vary with the curvature of the substrate. Moreover, during the mathematical calculations, A must be equal to the target value A_0 , indicating that the contribution of the energy resulting from the surface tension is zero (see Eq. (2) and Eq. (S2) in the Supplemental Material [42]).

Specifically, for a vesicle adhered to a spherical substrate with curvature radius R (Fig. 1), we have the following relations,

$$\begin{aligned} L_1(\psi) &= \left[\frac{1}{2} \left(\pm \frac{2}{R} - c_0 \right)^2 + \frac{\sigma - w}{k_c} \right] R \sin \psi \\ &+ \frac{\Delta P}{2k_c} R^2 \sin^3 \psi, \quad (3) \\ L(\psi, \dot{\psi}, r, \dot{r}, z, \dot{z}) &= \frac{1}{2} \left(\dot{\psi} + \frac{\sin \psi}{r} - c_0 \right)^2 r \\ &+ \frac{\sigma}{k_c} r + \frac{\Delta P}{2k_c} r^2 \sin \psi \\ &+ \mu(s)(\dot{r} - \cos \psi) + \eta(s)(\dot{z} - \sin \psi), \end{aligned} \quad (4)$$

where $L_1(\psi)$ and $L(\psi, \dot{\psi}, r, \dot{r}, z, \dot{z})$ represent the functions of the energy densities of the contact region and the free area, respectively; $\mu(s) = \bar{\mu}(s)/(2\pi k_c)$; and $\eta(s) = \bar{\eta}(s)/(2\pi k_c)$. Since both concave and convex substrates are here considered, on the right-hand side of Eq. (3), we employ the plus and minus signs to describe the cases shown in Figs. 1(a) and 1(b), respectively.

Next, by minimizing the free energy in Eq. (2) [38], we obtain the equilibrium equation for the free surface of the vesicle, as well as the boundary conditions. Since k_c is constant, for simplicity, we carry out the first variation of $E_{\text{tot}}/(2\pi k_c)$ instead of E_{tot} . Then, we have

$$\begin{aligned} \delta \left(\frac{E_{\text{tot}}}{2\pi k_c} \right) &= L_1|_{s_0} \delta s_0 - \int_{s_0}^{s_0+\delta s_0} L ds + \int_{s_1}^{s_1+\delta s_1} L ds \\ &+ \int_{s_0}^{s_1} [L(\psi + \delta\psi, \dot{\psi} + \delta\dot{\psi}, r + \delta r, \dot{r} + \delta\dot{r}, z + \delta z, \dot{z} + \delta\dot{z}) - L(\psi, \dot{\psi}, r, \dot{r}, z, \dot{z})] ds \\ &= L_1|_{s_0} \delta s_0 - L|_{s_0} \delta s_0 + L|_{s_1} \delta s_1 + \left(\frac{\partial L}{\partial \psi} \delta\psi \right) \Big|_{s_0}^{s_1} + \left(\frac{\partial L}{\partial \dot{\psi}} \delta\dot{\psi} \right) \Big|_{s_0}^{s_1} + \left(\frac{\partial L}{\partial r} \delta r \right) \Big|_{s_0}^{s_1} + \left(\frac{\partial L}{\partial \dot{r}} \delta\dot{r} \right) \Big|_{s_0}^{s_1} + \left(\frac{\partial L}{\partial z} \delta z \right) \Big|_{s_0}^{s_1} + \int_{s_0}^{s_1} \left[\left(\frac{\partial L}{\partial \psi} - \frac{d}{ds} \frac{\partial L}{\partial \dot{\psi}} \right) \delta\psi \right. \\ &\left. + \left(\frac{\partial L}{\partial r} - \frac{d}{ds} \frac{\partial L}{\partial \dot{r}} \right) \delta r + \left(\frac{\partial L}{\partial z} - \frac{d}{ds} \frac{\partial L}{\partial \dot{z}} \right) \delta z + \frac{\partial L}{\partial \mu} \delta\mu + \frac{\partial L}{\partial \eta} \delta\eta \right] ds + \frac{1}{2\pi k_c} \left(\int_0^{s_1} 2\pi r ds - A_0 \right) \delta\sigma, \end{aligned} \quad (5)$$

where δs_0 and δs_1 denote the increments of s_0 and s_1 , respectively; and $\delta\psi$, δr , δz , $\delta\mu$, and $\delta\eta$ are the first variations of $\psi(s)$, $r(s)$, $z(s)$, $\mu(s)$, and $\eta(s)$, respectively.

B. Governing equations

The equilibrium differential equations of the free surface and the relevant boundary conditions are given, with the tedious derivations available in the Supplemental Material [42]. The first variation of $E_{\text{tot}}/(2\pi k_c)$ leads to a set of Euler-Lagrange equations that govern the free surface of the adhered vesicle:

$$\ddot{\psi} + \dot{\psi} \frac{\cos \psi}{r} - \frac{\sin 2\psi}{2r^2} - \frac{\Delta P}{2k_c} r \cos \psi - \mu(s) \frac{\sin \psi}{r} + \eta(s) \frac{\cos \psi}{r} = 0, \quad (6)$$

$$\frac{1}{2} \left[(\dot{\psi} - c_0)^2 - \left(\frac{\sin \psi}{r} \right)^2 \right] + \frac{\sigma}{k_c} + \frac{\Delta P}{k_c} r \sin \psi - \dot{\mu}(s) = 0, \quad (7)$$

$$\dot{\eta}(s) = 0, \quad (8)$$

$$\dot{r} - \cos \psi = 0, \quad (9)$$

$$\dot{z} - \sin \psi = 0. \quad (10)$$

The boundary conditions are

$$\dot{\psi}_{s_0} = \pm \frac{1}{R} + \sqrt{\frac{2w}{k_c}}, \quad (11)$$

$$\mu_{s_0} \cos \psi_{s_0} = -\frac{1}{2} \left[\dot{\psi}_{s_0}^2 - \left(\pm \frac{1}{R} - c_0 \right)^2 \right] R \sin \psi_{s_0} + \frac{\sigma}{k_c} R \sin \psi_{s_0} + \frac{\Delta P}{2k_c} R^2 \sin^3 \psi_{s_0}, \quad (12)$$

$$\mu_{s_1} = 0, \quad (13)$$

$$\eta_{s_0} = 0, \quad (14)$$

$$\eta_{s_1} = 0, \quad (15)$$

where ψ_{s_0} , $\dot{\psi}_{s_0}$, μ_{s_0} , μ_{s_1} , η_{s_0} , and η_{s_1} are the values of $\psi(s)$, $\dot{\psi}(s)$, $\mu(s)$, $\mu(s)$, $\eta(s)$, and $\eta(s)$ at points s_0 and s_1 , respectively. It is emphasized that on the right-hand sides of Eqs. (11) and (12), the plus and minus signs denote the cases of a vesicle adhered to a spherical concave [Fig. 1(a)] and a spherical convex [Fig. 1(b)] substrate, respectively [17,21].

Since it is difficult to analytically solve the above differential equations, we numerically solve them by using a shooting method (Sec. 3 in the Supplemental Material [42]). Then the configuration of a vesicle and the energy of different parts can be determined. For simplicity, the following dimensionless parameters are employed,

$$\begin{aligned} \bar{L} &= \frac{L}{R_0}, \quad \bar{A} = \frac{A}{R_0^2}, \quad \bar{V} = \frac{V}{R_0^3}, \quad \bar{\kappa} = \kappa R_0, \quad \bar{k}_c = \frac{k_c}{k_{c0}}, \quad \bar{w} \\ &= \frac{w R_0^2}{k_{c0}}, \quad \bar{\sigma} = \frac{\sigma R_0^2}{k_{c0}}, \quad \bar{\Delta P} = \frac{\Delta P R_0^3}{k_{c0}}, \quad \bar{E} = \frac{E}{k_{c0}}, \end{aligned} \quad (16)$$

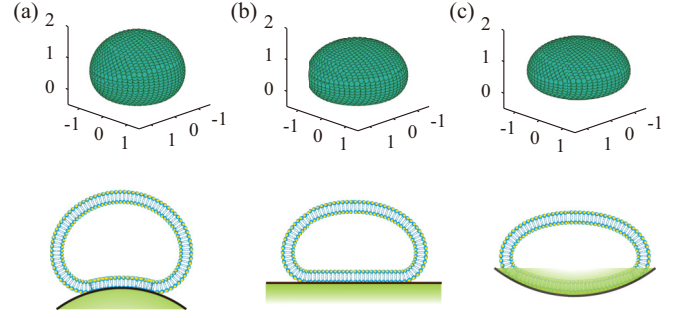


FIG. 2. Configuration of vesicles adhered to spherical substrates with different curvature radii. (a) $\bar{\kappa} = -0.5$ ($\bar{R} = 2$); (b) $\bar{\kappa} = 0$ ($\bar{R} = \infty$); (c) $\bar{\kappa} = 0.4$ ($\bar{R} = 2.5$). The upper panel shows the three-dimensional configurations from an oblique side view, and the lower panel shows the corresponding profiles from a side view. The configurations of the vesicle in the upper and lower panels are drawn to scale, respectively, while the lipid molecules are drawn not to scale compared with the vesicles.

where R_0 is a characteristic length, defined as $R_0 = [A_0/(4\pi)]^{1/2}$ (the typical size of vesicles or cells varies between 0.1 and several tens of micrometers [48,49]). $\bar{A}_0 = 4\pi$ is assumed for all vesicles in the following analysis. In Eq. (16), as aforementioned, κ denotes the mean curvature of the substrate. It is stressed that for a general curved substrate with an arbitrary shape, each point may have a different mean curvature. Here, κ is defined as the mean curvature of the geometric center of the contact region, which is positive and negative on concave and convex substrates, respectively. In addition, k_{c0} is a characteristic stiffness (typically on the order of $\sim 10^{-19}$ J) [50] and it is a constant.

III. RESULTS AND DISCUSSIONS

A. Numerical results

As shown in Fig. 2, the equilibrium configurations of the vesicle on curved spherical substrates are investigated. First, to examine the curvature effect, we exemplarily choose $\bar{\kappa} = -0.5$ ($\bar{R} = 2$), $\bar{\kappa} = 0$ ($\bar{R} = \infty$), and $\bar{\kappa} = 0.4$ ($\bar{R} = 2.5$), corresponding to the convex, flat, and concave substrates shown in Figs. 2(a)–2(c), respectively. Second, some basic dimensionless parameters are given as $\bar{k}_c = 1$, $\bar{c}_0 = 0$, $\bar{w} = 6$, and $\bar{\Delta P} = 4$. Lastly, the two unknown parameters $\bar{\sigma}$ and \bar{V} can be obtained based on the shooting method (see Sec. 3 in the Supplemental Material [42]), and the numerical solutions are $\bar{\sigma} = -1.61$ and $\bar{V} = 3.99$ when $\bar{\kappa} = -0.5$, $\bar{\sigma} = -0.8$ and $\bar{V} = 3.68$ when $\bar{\kappa} = 0$, and $\bar{\sigma} = 0.23$ and $\bar{V} = 3.68$ when $\bar{\kappa} = 0.4$. These results suggest that despite some parameters (i.e., \bar{A}_0 , \bar{k}_c , \bar{c}_0 , \bar{w} , and $\bar{\Delta P}$) being kept, the shape and the other parameters (i.e., $\bar{\sigma}$ and \bar{V}) of the vesicle are determined by the mean curvature of the adhesion region. Moreover, as shown in the lower panel of Fig. 2 (from left to right), the dimensionless adhesion area \bar{A}_c monotonously increases with the dimensionless mean curvature $\bar{\kappa}$ of the adhesion region, which will be discussed in detail in Sec. IV.

Besides the equilibrium configurations of the vesicle, we are also interested in the dependence of its total free energy \bar{E}_{tot} on the mean curvature of the adhesion region $\bar{\kappa}$.

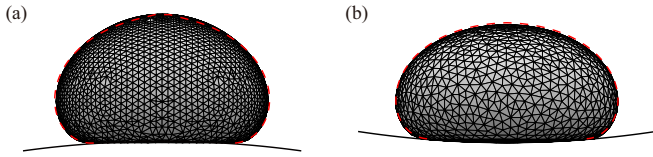


FIG. 3. Vesicle configuration obtained by employing SURFACE EVOLVER (SE), and comparison between the results of SE (domain with grid) and theory (dashed red curve). (a) A vesicle on a concave substrate with $\bar{k}_c = 1$, $\bar{c}_0 = 0$, $\bar{w} = 6$, $\Delta\bar{P} = 4$, and $\bar{\kappa} = -0.1$; (b) a vesicle on a convex substrate with $\bar{k}_c = 1$, $\bar{c}_0 = 0$, $\bar{w} = 6$, $\Delta\bar{P} = 4$, and $\bar{\kappa} = 0.1$.

Remarkably, it is found that \bar{E}_{tot} monotonously decreases with $\bar{\kappa}$, and $\bar{E}_{tot} = 41.1$, $\bar{E}_{tot} = 36.6$, and $\bar{E}_{tot} = 29.2$ are obtained for the cases in Figs. 2(a)–2(c), respectively. This tendency is consistent with the curvature-dependent wetting behavior of drops [30–33]. However, until now we have only obtained the configurations of vesicle and substrate that both have axisymmetric shapes (Fig. 2); a thorough investigation of the adhesion behavior of vesicle on complex curved substrates will be the next objective.

Since it is difficult to analytically solve the configurations of the vesicle with an arbitrary shape, we perform FEM simulations by employing the public domain software package SURFACE EVOLVER (SE) [51]. The basic concept of SE is to minimize the energy and find the equilibrium shape of a liquid volume surface with given parameters such as the surface tension and stiffness, subjected to external forces (e.g., gravity, centrifugal force, magnetic force) and constraints (e.g., volume conservation, contact angle, pinning of the contact line). SE has been widely applied to studying various interfacial phenomena (such as morphologies of droplets and particles [30,52–55], foams [56], etc.), as well as the equilibrium

configuration of biomembranes [57,58], with excellent agreement to experimental results.

First, to check its reliability, the SE method is employed to simulate the morphology of the axisymmetric vesicles which have already been solved theoretically. Then, comparisons between the theoretical and simulation results are carried out. As shown in Figs. 3(a) and 3(b), we exemplarily exhibit two vesicles adhered to a convex and a concave substrate, respectively, where the red curves represent the theoretical results, and the domains with grids represent the simulation results. The comparisons suggest a very good consistency.

Next, to achieve a general perspective, we consider non-axisymmetric vesicles and substrates. Figure 4 shows the adhesion of vesicles on cylindrical, conical, and saddle-shaped substrates. By varying the radius of the cylindrical substrate, as well as placing the vesicle at different places on the conical substrate, the value of $\bar{\kappa}$ is systematically varied. For the saddle-shaped substrate, we study the case when the vesicle adheres to the saddle point of the substrate, where the mean curvature $\bar{\kappa}$ is systematically varied by designing substrates with different shapes. Moreover, the vesicles are placed on the outside and inside of these curved substrates, and thus both the negative and positive mean curvatures are considered.

As shown in Fig. 5, the red squares, green stars, and cyan pentagons are simulation results obtained by SE on cylindrical, conical, and saddle-shaped substrates, respectively. We also give the theoretical (blue dots) and simulation results (orange diamonds) on spherical substrates. The scenario of Fig. 5 is reminiscent of the curvature-driven phenomenon of drops [30], and the following conclusions can be drawn: (1) All the data collapse onto a master curve (i.e., the red dashed curved); (2) it suggests that the total free energy of the adhered vesicles depends mainly on the mean curvature of the adhesion region

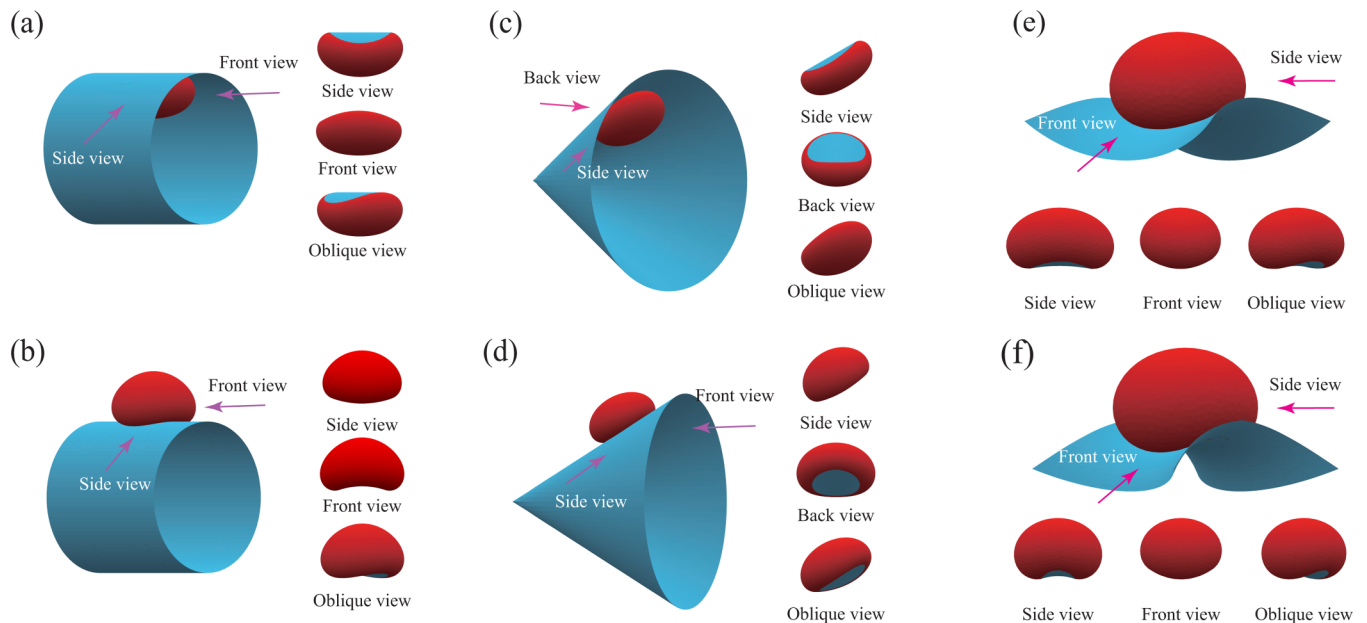


FIG. 4. Different views of vesicles adhered to the inner and outer sides of the cylindrical, conical, and saddle-shaped substrates carried out by SE simulations: (a) $\bar{\kappa} = 0.25$, (b) $\bar{\kappa} = -0.25$, (c) $\bar{\kappa} = 0.19$, (d) $\bar{\kappa} = -0.19$, (e) $\bar{\kappa} = 0.25$, and (f) $\bar{\kappa} = -0.25$. The red and light blue colors represent the free area and adhered region, respectively.

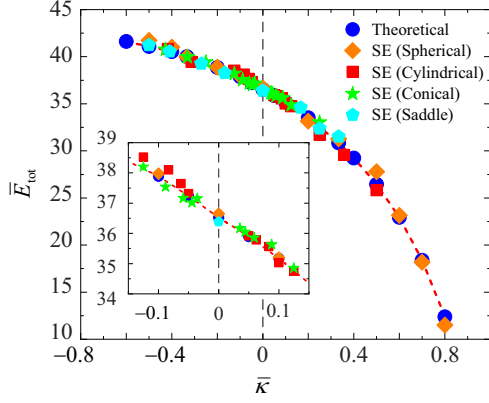


FIG. 5. Dimensionless free energy \bar{E}_{tot} as a function of the substrate mean curvature $\bar{\kappa}$. Different kinds of substrates (spherical, cylindrical, conical, and saddle-shaped) are compared. The blue dots represent the theoretical results of the vesicles on spherical substrates, and the orange diamonds, red squares, green stars, and cyan pentagons represent the SE results on the spherical, cylindrical, conical, and saddle-shaped substrates, respectively. $\bar{k}_c = 1$, $\bar{c}_0 = 0$, $\bar{w} = 6$, $\bar{A} = 4\pi$, and $\Delta\bar{P} = 4$ are physical parameters with fixed values. The inset is a zoomed-in view of energy \bar{E}_{tot} around $\bar{\kappa} = 0$, which demonstrates a linear relation.

but is insensitive to the specific shape of the substrate; (3) a zoomed-in view of the energy \bar{E}_{tot} around $\bar{\kappa} = 0$ is given, which demonstrates a linear relation.

Moreover, Fig. 6 gives the variations of the components of the total free energy with respect to the mean curvature (in dimensionless forms). Specifically, the dimensionless adhesion energy $\bar{E}_{\text{adh}} = -\bar{w}\bar{A}_c$ (red square dots) has a negative value and it monotonously decreases with $\bar{\kappa}$. However, the dimensionless stiffness energy \bar{E}_κ first increases and then slightly decreases with $\bar{\kappa}$, whereas the dimensionless volume potential \bar{E}_V has an opposite tendency and its variation with $\bar{\kappa}$ is negligible. Since the amplitude of the variation of \bar{E}_{adh} is remarkably larger than \bar{E}_κ and \bar{E}_V , this suggests that \bar{E}_{adh} plays

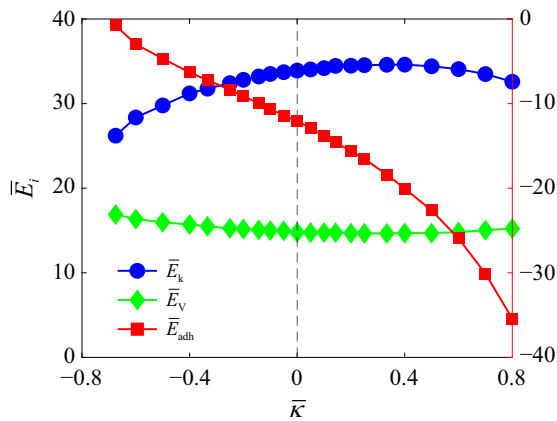


FIG. 6. Variation of the relevant energy as functions of the dimensionless mean curvature $\bar{\kappa}$ of the adhesion region. The blue dots, green diamonds, and red squares represent the dimensionless stiffness energy \bar{E}_κ , volume potential \bar{E}_V , and adhesion energy \bar{E}_{adh} , respectively. $\bar{k}_c = 1$, $\bar{c}_0 = 0$, $\bar{w} = 6$, $\bar{A} = 4\pi$, and $\Delta\bar{P} = 4$ are dimensionless physical parameters with fixed values.

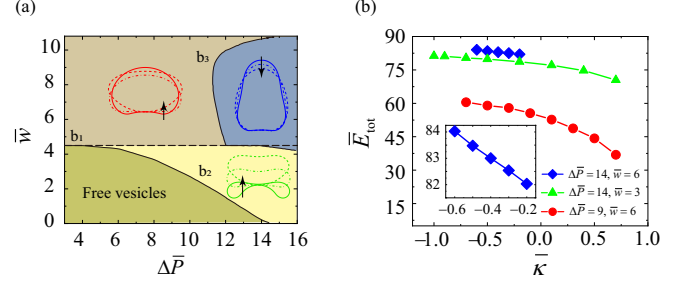


FIG. 7. Adhered shape of vesicle and curvature-dependent energy. Here, $\bar{k}_c = 1$, $\bar{c}_0 = 0$, and $\bar{A} = 4\pi$. (a) Bound-unbound shape transformation in the $\bar{w} - \Delta\bar{P}$ parameter space for concave substrates with fixed values of $\bar{\kappa} = 0.5$ (and $\bar{R} = 2$). b_1 (dashed curve), b_2 (solid curve), and b_3 (solid curve) are defined as the transition lines and are revisited based on the work of Das and Du [17], which divides the parameter space into three regions with three kinds of adhering vesicle: bound spherical state (red curve), bound oblate state (green), and bound prolate state (blue). If \bar{k}_c , \bar{c}_0 , and \bar{A} are fixed but $\bar{\kappa}$ is increased, different $\bar{w} - \Delta\bar{P}$ parameter spaces will be obtained, and the evolution of each kind of vesicle follows the corresponding arrows. (b) Dimensionless free energy \bar{E}_{tot} as a function of $\bar{\kappa}$ for these three kinds of vesicle. The dots are numerical results with corresponding colors of the vesicles shown in (a). The inset is a zoomed-in view of the bound prolate state.

a significant role accounting for the variation of the energy of the system.

Furthermore, we systematically elaborate upon the influences of other parameters (i.e., \bar{w} , \bar{c}_0 , and \bar{k}_c) on the variation of the relevant energies (i.e., the total energy \bar{E}_{tot} and its components such as \bar{E}_{adh} , \bar{E}_V , and \bar{E}_κ) of the adhered vesicle in terms of the mean curvature $\bar{\kappa}$, and we put these investigations in Sec. 5 of the Supplemental Material [42]. In all of these cases, \bar{E}_{tot} decreases with $\bar{\kappa}$, which confirms that the mean curvature-dependent adhesion behavior is general and not substantially influenced by the physical parameters.

B. Adhered shapes

In the above analysis, the mean curvature-dependent adhesion of vesicles has been revealed. Previous studies showed that vesicle shape transformation induced by the adhesion could happen even on planar substrates [16]. In this section, by considering a larger range of parameters (thus the vesicle would have different kinds of shapes, in other words, adhering states), we will shine more light on the generality of the curvature-dependent adhesion.

As early as 30 years ago, Seifert *et al.* discussed the shape transformation of free vesicles [59] and vesicles adhering to planar surfaces [16]. After that, Das and Du investigated the shape transformation of adhering vesicles on curved substrates in the $\bar{w} - \Delta\bar{P}$ parameter space [17]. As in the example shown in Fig. 7(a), the $\bar{w} - \Delta\bar{P}$ parameter space of a vesicle adhered on a concave substrate with $\bar{\kappa} = 0.5$ (and $\bar{R} = 2$) is revisited based on the work of Das and Du [17]. According to the conclusion of Das and Du [17], b_1 (dashed line), b_2 (solid curve), and b_3 (solid curve) represent the transition lines and divide the $\bar{w} - \Delta\bar{P}$ parameter space into three regions with bound spherical (red color), bound oblate

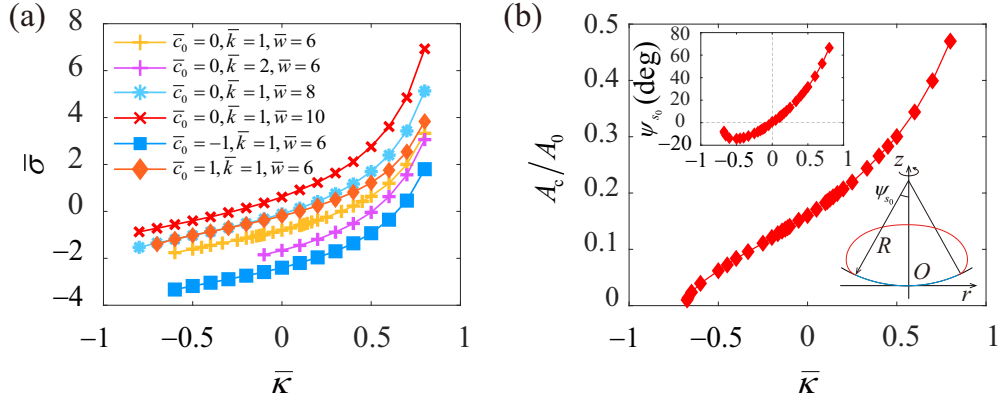


FIG. 8. Relations of $\bar{\sigma}$ vs $\bar{\kappa}$ and A_c/A_0 vs $\bar{\kappa}$. (a) $\bar{A} = 4\pi$ and $\Delta\bar{P} = 4$ are constant parameters. The other parameters for each curve are listed in the legend; (b) $\bar{k}_c = 1$, $\bar{c}_0 = 0$, $\bar{w} = 6$, $\bar{A} = 4\pi$, and $\Delta\bar{P} = 4$ are constant parameters, corresponding to the case of Fig. 5.

(green color), and bound prolate (blue color) states of the vesicle, respectively. Moreover, these transition lines (i.e., b_1 , b_2 , and b_3) in the $\bar{w} - \Delta\bar{P}$ parameter space change with the substrate curvature, and if $\bar{\kappa}$ increases, the vesicle shape varies following the accompanying arrows [see the insets of Fig. 7(a)]. Moreover, the relations between the dimensionless total energy \bar{E}_{tot} and the mean curvature $\bar{\kappa}$ of the adhesion region in these different cases are also investigated, and their mean curvature-dependent adhesion behaviors are confirmed in Fig. 7(b). Since the scope of $\bar{\kappa}$ for the bound prolate state is pretty narrow, its curvature-dependent adhesion behavior is presented by a zoomed-in view as the inset of Fig. 7(b).

Here, it is emphasized that this work aims at revealing the mean curvature-dependence of the total free energy of the adhered vesicle, and we will not investigate the shape transformation of a vesicle induced by the mean curvature of a substrate having complex shapes, which is beyond the scope of the present paper and deserves a dedicated study in the future. For axisymmetric shapes of substrate and vesicle, how substrate curvature triggers the shape transformation of a vesicle can be found in the work of Das and Du [17].

IV. DISCUSSIONS

From the above analysis, we have obtained the following conclusions that are worth discussing. The total free energy of the adhered vesicle depends mainly on the mean curvature of the adhesion region but is insensitive to the specific shape of the substrate, which is supported by Fig. 5 where the total free energy of the adhered vesicles on different substrates collapses onto a master curve. This finding is similar to the curvature-dependent wetting behavior of drops on curved substrates [30–33]. Moreover, for vesicles with various shapes as shown in Fig. 7, it also shows a monotonous decrease of the total energy with the mean curvature. Considering that the vesicle is widely employed as a simple model for cell membranes [17], in the following, we will discuss the above results of vesicle adhesion that may correlate to the previously reported biological experiments of cells.

The first insight is about the main conclusion shown in Fig. 5, that the total free energy decreases with the mean curvature of the adhesion region, which indicates that spontaneous motion of a vesicle may happen when adhering on

a substrate with a mean curvature gradient. In the experimental work of Pieuchot *et al.* [2], it is observed that for mesenchymal stem cells (MSCs) adhering on a sinusoidal substrate, the adherent cells avoid convex regions during their migration and position themselves in concave valleys. In this regard, our mean curvature-dependent energy may give some perspectives to understanding the cell migration behavior: the free energy of the adhering cell on the concave substrate is higher than it is on the convex substrate, which leads to a spontaneous cell migration to decrease the energy of the cell.

Moreover, considering the mean curvature-dependent surface tension and configuration of the vesicle, we will qualitatively compare our results with the experimental observations of human mesenchymal stem cells (hMSCs) adhering on spherical substrates carried out by Werner *et al.* [3]. A spiderlike morphology of cell on concave substrates was reported, while there was a snaillike morphology on convex substrates. To adopt the spiderlike morphology, the cell has to stretch with tensile elements to lift cells on the concave substrates. On the contrary, to adopt the snaillike morphology, the cell has to bend to attach to the convex substrates. Therefore, stronger actin filaments were observed on concave substrates than on convex substrates. In the experiments of Werner *et al.* [3], the stronger actin filament means a stronger tensile force, which corresponds to a larger value of surface tension in our result. As shown in Fig. 8(a), for each specific curve, the surface tension indeed increases with the mean curvature of the adhesion region. It should be stressed that the real situation of cell adhesion is more complicated; for instance, the adhesive process involves assembly and disassembly of the cytoskeleton [60], which has not been considered in our model. Therefore, we are not able to correlate our dimensionless analysis to the exact value of the surface tension. In addition, we note that for different parameter sets, the sign of the surface tension would change with the mean curvature; its biological meanings remain to be addressed. Therefore, more elaborate theories need to be developed in the future.

Finally, as shown in Fig. 8(b), it is worth exploring further how much contact area of the adhering vesicle there is on the curved substrate, and its significance on biofouling. For a given parameter set ($\bar{k}_c = 1$, $\bar{c}_0 = 0$, $\bar{w} = 6$, $\bar{A} = 4\pi$, and $\Delta\bar{P} = 4$), relations of A_c/A_0 vs $\bar{\kappa}$ and $2\psi_s$ vs $\bar{\kappa}$ are given. Here, $2\psi_s$ is defined as the central angle of the contact area

and its geometrical meaning is illustrated in the inset. Moreover, the sign of $2\psi_{s_0}$ is defined as positive and negative on the concave and convex substrates, respectively (more details are given in Fig. S1 of the Supplemental Material [42]). We can see that $2\psi_{s_0}$ first decreases and then increases with $\bar{\kappa}$. On the convex substrate ($\bar{\kappa} < 0$), generally, the absolute value of α is much smaller than it is on the concave substrate ($\bar{\kappa} > 0$). On the one hand, Fig. 8(b) suggests that the concave substrate facilitates adhesion, while the adhesion is suppressed on the convex substrate. On the other hand, it is interesting to see that when the mean curvature of the adhesion region is smaller than a critical value, there is no solution of the configuration of the adhering vesicle, which means that adhesion could hardly happen. Recently, Vellwock and Yao [61] gave the relation between the dimensions of the effective antifouling topographies and the dimensions of the prevented bio-foulers. According to their statistical results, some antifouling substrates, such as shark skin [62], sea stars [63], and crabs [64], have the structure of bumps (i.e., convex structures with negative curvatures) with similar dimensions as their bio-foulers. Therefore, such antifouling property benefits from the convex substrate with a much smaller negative mean curvature. In this regard, we hope our perspective would not only offer greater understanding of some antifouling structured substrates but also would be helpful to optimize the design of antifouling materials, which have been widely used in microfluidics, medical and biotechnology, and marine engineering [12].

V. CONCLUSIONS

In the present work, we have systematically investigated the influence of the substrate mean curvature on the adhesion of vesicles with a constant area. It is discovered that the total energy of an adhering vesicle depends mainly on the mean curvature of the adhesion region but is insensitive to the specific shape of the substrate. FEM simulations help us understand the adhesion behavior of vesicles on substrates with complex shapes, and the results show that the total energy monotonously decreases with the mean curvature of the adhesion region. However, open questions remain to be further explored. For example, though the effect of the mean curvature has been illustrated in Fig. 5, it will be valuable to derive an analytical solution which can explicitly quantify the relation between the energy and the mean curvature when it is close to zero. Experiments are critically important and need to be carried out to provide more evidence for the above conclusions. In addition, shape transformation of vesicles induced by the substrate curvature on general surfaces also deserves a dedicated study.

ACKNOWLEDGMENT

Support from the National Natural Science Foundation of China (Grants No. 11872227, No. 12032014, No. 11921002, and No. 11902179) is gratefully acknowledged.

There are no conflicts of interest to declare.

-
- [1] A. J. B. Alberts, J. Lewis, M. Raff, K. Roberts, and P. Walter, *Molecular Biology of the Cell*, 4th ed. (Garland Science, New York, 2002).
- [2] L. Pieuchot, J. Marteau, A. Guignandon, T. D. Santos, I. Brigaud, P. Chauvy, T. Cloatre, A. Ponche, T. Petithory, P. Rougerie *et al.*, Curvotaxis directs cell migration through cell-scale curvature landscapes, *Nat. Commun.* **9**, 3995 (2018).
- [3] M. Werner, S. B. G. Blanquer, S. P. Haimi, G. Korus, J. W. C. Dunlop, G. N. Duda, D. W. Grijpma, and A. Petersen, Surface curvature differentially regulates stem cell migration and differentiation via altered attachment morphology and nuclear deformation, *Adv. Sci.* **4**, 1600347 (2017).
- [4] Y. Yang and H. Jiang, Shape and dynamics of adhesive cells: mechanical response of open systems, *Phys. Rev. Lett.* **118**, 208102 (2017).
- [5] X. Zhou, S. Zhao, X. Zhai, K. Zhang, H. Chen, and S. Zhang, Phase diagram of a tubular vesicle adhering between two parallel rigid planes, *Phys. Rev. E* **93**, 042801 (2016).
- [6] X. Yi, X. H. Shi, and H. J. Gao, Cellular Uptake of Elastic Nanoparticles, *Phys. Rev. Lett.* **107**, 098101 (2011).
- [7] K. Anselme, N. T. Wakhloo, P. Rougerie, and L. Pieuchot, Role of the nucleus as a sensor of cell environment topography, *Adv. Healthcare Mater.* **7**, 1701154 (2018).
- [8] S. Amorim, C. A. Reis, R. L. Reis, and R. A. Pires, Extracellular matrix mimics using hyaluronan-based biomaterials, *Trends Biotechnol.* **39**, 90 (2021).
- [9] X. Yi and H. J. Gao, Phase diagrams and morphological evolution in wrapping of rod-shaped elastic nanoparticles by cell membrane: A two-dimensional study, *Phys. Rev. E* **89**, 062712 (2014).
- [10] J. Zonderland and L. Moroni, Steering cell behavior through mechanobiology in 3D: a regenerative medicine perspective, *Biomaterials* **268**, 120572 (2021).
- [11] A. A. Khalili and M. R. Ahmad, A review of cell adhesion studies for biomedical and biological applications, *Int. J. Mol. Sci.* **16**, 18149 (2015).
- [12] T. T. Lee, J. R. García, J. I. Paez, A. Singh, E. A. Phelps, S. Weis, Z. Shafiq, A. Shekaran, A. del Campo, and A. J. García, Light-triggered in vivo activation of adhesive peptides regulates cell adhesion, inflammation and vascularization of biomaterials, *Nat. Mater.* **14**, 352 (2015).
- [13] W. Barthlott, M. Mail, and C. Neinhuis, Superhydrophobic hierarchically structured surfaces in biology: evolution, structural principles and biomimetic applications, *Philos. Trans. R. Soc. A* **374**, 20160191 (2016).
- [14] R. S. Lipowsky and U. Seifert, Adhesion of membranes: a theoretical perspective, *Langmuir* **7**, 1867 (1991).
- [15] U. Seifert, Adhesion of vesicles in two dimensions, *Phys. Rev. A* **43**, 6803 (1991).
- [16] U. Seifert and R. Lipowsky, Adhesion of vesicles, *Phys. Rev. A* **42**, 4768 (1990).
- [17] S. Das and Q. Du, Adhesion of vesicles to curved substrates, *Phys. Rev. E* **77**, 011907 (2008).
- [18] C. Lv, Y. Yin, and J. Yin, Geometric theory for adhering lipid vesicles, *Colloids Surf., B* **74**, 380 (2009).
- [19] U. Seifert, Configurations of fluid membranes and vesicles, *Adv. Phys.* **46**, 13 (1997).

- [20] R. Capovilla and J. Guven, Geometry of lipid vesicle adhesion, *Phys. Rev. E* **66**, 041604 (2002).
- [21] R. Lipowsky, Understanding giant vesicles: a theoretical perspective, in *The Giant Vesicle Book*, edited by R. Dimova and C. M. Marques (CRC Press, Taylor & Francis Group, Boca Raton, FL, 2020), pp. 73–168.
- [22] J. Zhang, S. Das, and Q. Du, A phase field model for vesiclesubstrate adhesion, *J. Comput. Phys.* **228**, 7837 (2009).
- [23] W. D. Shi, X. Q. Feng, and H. J. Gao, Two-dimensional model of vesicle adhesion on curved substrates, *Acta Mech. Sin.* **22**, 529 (2006).
- [24] X. H. Zhou, J. L. Liu, and S. L. Zhang, Adhesion of a vesicle on an elastic substrate: 2D analysis, *Colloids Surf., B* **110**, 372 (2013).
- [25] S. Z. Lin, Y. Li, J. Ji, B. Li, and X. Q. Feng, Collective dynamics of coherent motile cells on curved surfaces, *Soft Matter* **16**, 2941 (2020).
- [26] W. Xi, S. Sonam, T. B. Saw, B. Ladoux, and C. T. Lim, Emergent patterns of collective cell migration under tubular confinement, *Nat. Commun.* **8**, 1517 (2017).
- [27] H. G. Yevick, G. Duclos, I. Bonnet, and P. Silberzan, Architecture and migration of an epithelium on a cylindrical wire, *Proc. Natl. Acad. Sci. USA* **112**, 5944 (2015).
- [28] J. Agudo-Canalejo and R. Lipowsky, Critical particle sizes for the engulfment of nanoparticles by membranes and vesicles with bilayer asymmetry, *ACS Nano* **9**, 3704 (2015).
- [29] J. Agudo-Canalejo and R. Lipowsky, Uniform and Janus-like nanoparticles in contact with vesicles: energy landscapes and curvature-induced forces, *Soft Matter* **13**, 2155 (2017).
- [30] C. Lv, C. Chen, Y. C. Chuang, F. G. Tseng, Y. Yin, F. Grey, and Q. Zheng, Substrate Curvature Gradient Drives Rapid Droplet Motion, *Phys. Rev. Lett.* **113**, 026101 (2014).
- [31] P. Galatola, Spontaneous capillary propulsion of liquid droplets on substrates with nonuniform curvature, *Phys. Rev. Fluids* **3**, 103601 (2018).
- [32] J. McCarthy, D. Vella, and A. A. Castrejon-Pita, Dynamics of droplets on cones: self-propulsion due to curvature gradients, *Soft Matter* **15**, 9997 (2019).
- [33] Y. Chen and X. Xu, Self-propulsion dynamics of small droplets on general surfaces with curvature gradient, *Phys. Fluids* **33**, 082107 (2021).
- [34] J. Liu, S. Li, and J. Hou, Near-post meniscus-induced migration and assembly of bubbles, *Soft Matter* **12**, 2221 (2016).
- [35] M. Cavallaro, L. Botto, E. P. Lewandowski, M. Wang, and K. J. Stebe, Curvature-driven capillary migration and assembly of rod-like particles, *Proc. Natl. Acad. Sci. USA* **108**, 20923 (2011).
- [36] Y. Yin, C. Chen, C. Lv, and Q. Zheng, Shape gradient and classical gradient of curvatures: driving forces on micro/nano curved surfaces, *Appl. Math. Mech. (Engl. Transl.)* **32**, 533 (2011).
- [37] P. G. de Gennes, F. Brochard-Wyart, and D. Quéré, *Capillarity and Wetting Phenomena: Drops and Bubbles and Pearls and Waves* (Springer-Verlag, New York, 2004).
- [38] M. Struwe, *Variational Methods*, 4th ed. (Springer, Berlin, 2008).
- [39] W. Helfrich, Elastic properties of lipid bilayers: theory and possible experiments, *Z. Naturforsch. C* **28**, 693 (1973).
- [40] Z. C. Ou-Yang, J. X. Liu, and Y. Z. Xie, *Geometric Methods in the Elastic Theory of Membranes in Liquid Crystal Phases* (World Scientific, Singapore, 1999).
- [41] D. J. Struik, *Lectures on Classical Differential Geometry*, 2nd ed. (Dover, New York, 1961).
- [42] See Supplemental Material at <http://link.aps.org/supplemental/10.1103/PhysRevE.107.024405> for detailed derivations, shooting method, surface evolver (se) simulation processes, and the influences of spontaneous curvature and stiffness, which includes Refs. [43–47].
- [43] K. Berndl, J. Kas, R. Lipowsky, E. Sackmann, and U. Seifert, Shape transformations of giant vesicles: extreme sensitivity to bilayer asymmetry, *Europhys. Lett.* **13**, 659 (1990).
- [44] V. Choudhary, G. Golani, A. S. Joshi, S. Cottier, R. Schneider, W. A. Prinz, and M. M. Kozlov, Architecture of lipid droplets in Endoplasmic Reticulum is determined by phospholipid intrinsic curvature, *Curr. Biol.* **28**, 915 (2018).
- [45] M. M. Kamal, D. Mills, M. Grzybek, and J. Howard, Measurement of the membrane curvature preference of phospholipids reveals only weak coupling between lipid shape and leaflet curvature, *Proc. Natl. Acad. Sci. USA* **106**, 22245 (2009).
- [46] G. T. Linke, R. Lipowsky, and T. Gruhn, Free fluid vesicles are not exactly spherical, *Phys. Rev. E* **71**, 051602 (2005).
- [47] R. Lipowsky and U. Seifert, Adhesion of vesicles and membranes, *Mol. Cryst. Liq. Cryst.* **202**, 17 (1991).
- [48] M. Chabanon and P. Rangamani, Gaussian curvature directs the distribution of spontaneous curvature on bilayer membrane necks, *Soft Matter* **14**, 2281 (2018).
- [49] M. Weiss, J. P. Frohnmayer, L. T. Benk, B. Haller, J. Janiesch, T. Heitkamp, M. Börsch, R. B. Lira, R. Dimova, R. Lipowsky *et al.*, Sequential bottom-up assembly of mechanically stabilized synthetic cells by microfluidics, *Nat. Mater.* **17**, 89 (2018).
- [50] T. Baumgart, S. T. Hess, and W. W. Webb, Imaging coexisting fluid domains in biomembrane models coupling curvature and line tension, *Nature (London)* **425**, 821 (2003).
- [51] K. Brakke, The surface evolver, *Exp. Math.* **1**, 141 (1992).
- [52] Y. S. Cho, G. R. Yi, J. M. Lim, S. H. Kim, V. N. Manoharan, D. Pine, and S. M. Yang, Self-organization of bidisperse colloids in water droplets, *J. Am. Chem. Soc.* **127**, 15968 (2005).
- [53] S. Crawford, S. K. Lim, and S. Gradedcak, Fundamental insights into nanowire diameter modulation and the liquid/solid interface, *Nano Lett.* **13**, 226 (2013).
- [54] I. Dević, J. M. E. Escobar, and D. Lohse, Equilibrium drop shapes on a tilted substrate with a chemical step, *Langmuir* **35**, 3880 (2019).
- [55] C. Lv and S. Hardt, Wetting of a liquid annulus in a capillary tube, *Soft Matter* **17**, 1756 (2021).
- [56] A. Kabla and G. Debregeas, Quasi-static rheology of foams, *J. Fluid Mech.* **587**, 23 (2007).
- [57] X. Michalet, Equilibrium shape degeneracy in starfish vesicles, *Phys. Rev. E* **76**, 021914 (2007).
- [58] A. Sakashita, N. Urakami, P. Zihlerl, and M. Imai, Three-dimensional analysis of lipid vesicle transformations, *Soft Matter* **8**, 8569 (2012).
- [59] U. Seifert, K. Berndl, and R. Lipowsky, Shape transformations of vesicles: phase diagram for spontaneous-curvature and bilayer-coupling models, *Phys. Rev. A* **44**, 1182 (1991).
- [60] T. D. Pollard and G. G. Borisy, Cellular motility driven by assembly and disassembly of actin filaments, *Cell* **112**, 453 (2003).

- [61] A. E. Vellwock and H. Yao, Biomimetic and bioinspired surface topographies as a green strategy for combating biofouling: a review, *Bioinspiration Biomimetics* **16**, 041003 (2021).
- [62] T. Sullivan and F. Regan, The characterization, replication and testing of dermal denticles of *Scyliorhinus canicula* for physical mechanisms of biofouling prevention, *Bioinspiration Biomimetics* **6**, 046001 (2011).
- [63] J. Guenther and R. De Nys, Surface microtopographies of tropical sea stars: lack of an efficient physical defence mechanism against fouling, *Biofouling* **23**, 419 (2007).
- [64] A. M. Brzozowska, F. J. Para-Velandia, R. Quintana, Z. Xiaoying, S. S. C. Lee, L. Chin-Sing, D. Jańczewski, S. L. M. Teo, and J. G. Vancso, Biomimicking micropatterned surfaces and their effect on marine biofouling, *Langmuir* **30**, 9165 (2014).